Online elemental characterization of collimated nanoaerosols by Laser-Induced Breakdown Spectroscopy of isolated particles

Cesar Alvarez-Llamas, Nathalie Herlin-Boime, Jean-Baptiste Sirven, Olivier Sublemontier

Online elemental characterization of collimated nanoaerosols by Laser-Induced Breakdown Spectroscopy of isolated particles

Cesar Alvarez-Llamas[1]; Nathalie Herlin-Boime[2] , Jean-Baptiste Sirven[3], Olivier Sublemontier[2]*

* olivier.sublemontier@cea.fr

[1] *Institut Lumière Matière (iLM), UMR5306, UCBL-CNRS; Villeurbanne, 69622, France*

[2] *Université Paris-Saclay, CEA, CNRS, NIMBE, 91191, Gif sur Yvette, 91191, France.*

[3] *Université Paris-Saclay, CEA, Service de Physico-Chimie, Gif-sur-Yvette 91191, France*

1 ABSTRACT

We present a new setup for the online elemental characterization of nanoaerosols during their gas-phase synthesis using Laser-Induced Breakdown Spectroscopy (LIBS). This system involves the interaction of a kHz rate pulsed laser with a collimated jet of particles under vacuum conditions (10^{-2} mbar), improving the LIBS detection capabilities. The low-pressure interaction reduces spectral line broadening, enhancing spectral resolution and eliminating background continuum from the laser-gas interaction. A sampling stage has also been incorporated into the design, enabling the continuous analysis of nanoaerosols during their high-throughput synthesis. This feature enhances the instrument's versatility and opens new possibilities for studying nanoparticle formation and properties in situ and in real-time.

The proof of concept was produced by an experiment of online elemental analysis of Li_2TiO_3 nanoparticles during their synthesis by laser pyrolysis. The monitoring of the LIBS emission signal of the particles in real time was demonstrated by measuring the signals from the three elements together with data conditional analysis to extract the events information. Moreover, the specific detection of Li signals was achieved in a single-nanoparticle detection mode, enabling to reach an absolute detection limit of 150 ag. The collimation step of particles in a jet, combined with a high repetition rate laser, opens the way to speciated monitoring of low-density aerosols in the sub-micrometer range.

2 INTRODUCTION

Over the past few decades, nanomaterials have gained significant importance, extending their application to a diverse array of disciplines, including their utilization for the fabrication of energy storage devices and having a key role in the latest advances in medical treatments or therapies.[1],[2] Manufactured nanoparticles are increasingly complex in their structure to combine multiple functionalities, leading to a complex determination of their characteristics, among them, the chemical composition, by traditional *ex-situ* methods of analysis. This difficulty arises due to labor-intensive sample preparation required for techniques such as X-ray Photoelectron Spectroscopy[3] or Inductively Coupled Plasma Mass Spectrometry, ICP-MS [4]. The requirements of the sampling steps might also induce a lack of representativeness of the analyzed part, which is a limit of e.g. Electronic Microscopies [5]. These methods may also be time-consuming, expensive, and *ex-situ*. Consequently, in-*situ* and real-time with reliable, fast, and non-invasive methods are preferable, but they should still be based on robust and previously tested chemical analysis techniques. An ideal analytical technique should combine multi-elemental analysis capability, allowing analysis under various conditions

with a high analysis rate and a simple sampling process, making it compatible with on-line monitoring of production processes.

Furthermore, nanoaerosols with anthropogenic or natural origins are omnipresent in the atmosphere, both indoors and outdoors. As a consequence, the ability to perform analysis by direct introduction of aerosol in the gas phase would be an added value to monitor continuously and effectively these micrometric and nanometric aerosols released into the atmosphere. In this regard, X-Ray Fluorescence technique is widely used, providing on-site elemental concentration of aerosol particles with portable instruments [6]. Nevertheless, it requires the deposition of relatively large quantities of material to perform the analysis, which is not compatible with ultrafine particle measurements. Furthermore, in the cases of light elements or low concentrations, the sensitivity of the real-time and *in-situ* nature of the method is questionable, and the size of the particles is still completely unknown. In order to estimate the size distribution, the Scanning Mobility Particle Sizer (SMPS) technique is widely used [7]. It combines a differential mobility analyzer with a particle counter and provides a number concentration as a function of the electrical mobility diameter from 2 to 1000 nm. Although this technique is very powerful, the real-time elemental composition of the particles remains out of reach.

Laser-Induced Breakdown Spectroscopy (LIBS) is an attractive alternative analytical technique for analyzing aerosols and particles. It is based on using a pulsed laser (typically, the pulse width is in the order of a few nanoseconds or below) to induce a transient plasma after irradiating the sample with enough fluence. Once the plasma is created, several processes take place (atomization, ionization, excitation, and recombination), emitting radiation at specific wavelengths, which allows the elemental characterization of the sample [8], [9]. Among the advantages of the technique, we may highlight the ability to analyze materials in any state of matter (solid, liquid, gas, or aerosol) in different atmospheric conditions, including a wide range of permissible pressures (10^{-9}-10^{2} bars), in different atmospheric compositions (air, Ar, He, N, Ne, etc.) [10]. In addition, LIBS allows in-situ and real-time analysis [11], including portable [12], remote [13], or laboratory LIBS applications.

The minimum amount of material required is also a crucial advantage of this technique for analyzing micro- and nano-aerosols. Added to the simultaneous multielemental detection capability, including light elements, this makes LIBS an interesting analytical technique. The use of LIBS for particulate materials has been investigated from early LIBS developments [14], with significant works made by Hahn and coworkers [15]-[20]. Furthermore, spectral identification of a single nanoparticle was demonstrated [21], with a mass detection limit in the tens of attograms range.

These benefits make it possible to analyze particle synthesis processes *in-situ*, online, and in real-time, or to monitor in the environment particles coming from anthropogenic sources. In this context, the use of LIBS together with a laser pyrolysis reactor has been reported by Amodeo et al. [22] as a promising laser-based tandem approach. However, the interaction of a laser with a non-confined particle cloud at ambient pressure implies drawbacks, including laser window clogging and spectral background from the gas phase, which makes the technique difficult to use in routine applications.

In the present work, we introduce the design of a robust instrument combining LIBS with an aerodynamic lens system to analyze particulate material. Evaluated with a source of aerosols from a laser pyrolysis system, the developed experimental setup is suitable for online, multielement analysis of particulate emissions in ambient air. The novel design encompasses various features that enhance overall performance and overcome the limitations of previous designs.

3 EXPERIMENTAL

The experimental setup was designed to achieve online elemental analysis of nanoaerosols by LIBS during their synthesis in the gas phase. The system included 3 stages: 1) particle sampling, 2) sample conditioning, and 3) sample analysis. Our experimental setup was connected to a particle synthesis setup, specifically a laser pyrolysis setup, which was custom-built in our laboratory [23]. Laser pyrolysis stands as a versatile technique extensively employed to produce substantial quantities of well-defined oxide and non-oxide nanopowders in the gas phase. Apart from traditional materials characterization methods, several aerosol-based techniques were previously used to characterize the particles produced by this process.[24] It was shown that particles produced by laser pyrolysis are highly agglomerated in chain-like agglomerates as soon as their diameter is less than a few tens of nm. Particles larger than 100 nm are mostly non-agglomerated, though a few large agglomerates could still remain.

For this study, Li_2TiO_3 particles were chosen as proof-of-concept samples for their relatively complex elemental composition, allowing the LIBS setup to evaluate multielement detection capabilities. The particles were synthesized continuously by laser pyrolysis of an atomized solution containing Lithium Nitrate dissolved in $C_6H_{18}N_2O_8Ti$ and water. The production rate was around 600 mg/h, and an average primary particle size of 120 nm was estimated by BET (Brunauer, Emett, Teller) surface area measurements. In this size range, low agglomeration of the primary particles was expected, though large-size agglomerates could still occasionally appear.

Throughout these experiments, we encountered two inevitable constraints. First, the LIBS analysis time is constrained in the specific case of Li_2TiO_3 particles by around 45 minutes of continuous operation due to the saturation of the particle collector in the synthesis process. Second, the physical separation between the pyrolysis setup and the analysis system, necessary for safety and laboratory arrangements, required the particles to travel inside a 6 mm internal diameter and 10 m long tube, leading to a slight delay of a few minutes between their entry into the sampling system and their detection. Consequently, the time that was actual available for analysis was less than 30 minutes.

3.1 PARTICLE SAMPLING

As illustrated in Figure 1, the sampling stage captures a controlled quantity of the particle flow directly from the synthesis reactor immediately after the synthesis process. The synthesized particle flow originated in the synthesis reactor and was vertically driven to the particle collector in a 40 mm-diameter tube. A 4 mm internal diameter sampling tube was horizontally placed in the main stream of particles, with a penetration distance of 5 mm in the 40 mm diameter tube of the synthesis reactor.

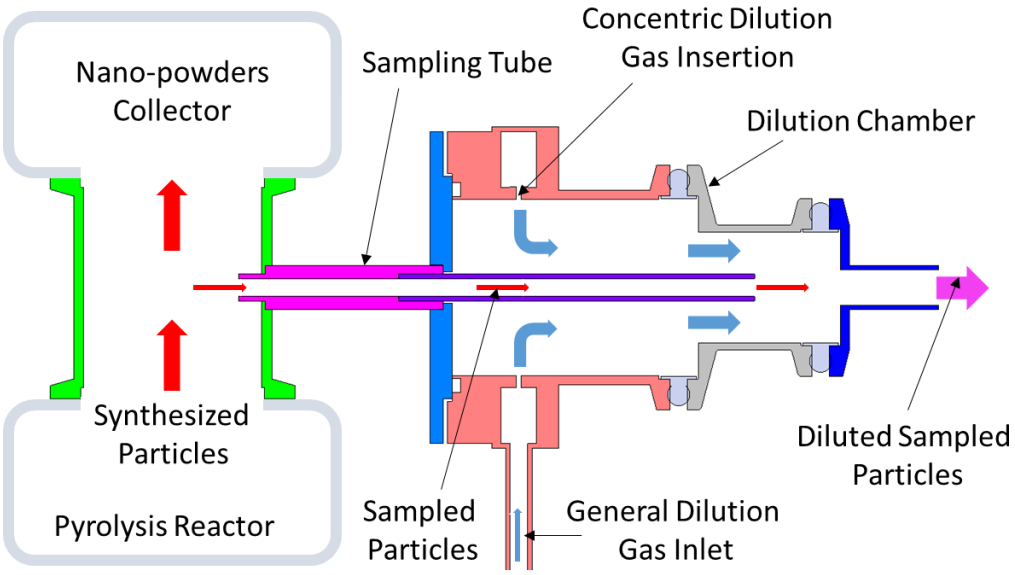

Figure 1: Diagram of the Sampling Stage principle and geometry.

Subsequently, the sampled particles were directed toward the sample conditioning stage. The particle sampling stage design included a dilution chamber to accommodate the high particle number and mass concentrations encountered at the reactor outlet. The sampling tube led to the dilution chamber, in which a dilution gas, typically argon, was inserted through 12 orifices of 1 mm diameter placed in a concentric way around the sampling tube. A distance of 20 mm from the sampling tube outlet to the dilution chamber outlet allowed the mixing of the samples to flow with the dilution gas before the exit of diluted sampled particles in an 8 mm internal diameter tube.

The flow rate of the diluted sample, fixed generally between 0.10 and 0.12 $l.min^{-1}$, was determined by the geometry of the sample conditioning stage, which was connected to a vacuum pump. By controlling the flow rate of the dilution gas between 50 - 100 % of the flow rate of the dilution sample, the dilution rate of the sampling stage was adjustable in a range of 50 to 99% and was generally adjusted between 80 and 90 % from the initial concentration in the synthesis reactor. Due to the high particle number concentration, a second dilution stage may be necessary in the case of an extremely high production rate synthesis. In this case, a commercial setup can be inserted after the sampling stage. In our sampling stage, the dilution part internal geometry was optimized by using CFD (Computational Fluid Dynamics) calculations to minimize particle loss in the sampling stage that may induce clogging of strategic parts. Examples of CFD calculations of nanosized particle trajectories are given in Figure 2 for 50% and 90% dilution in Ar.

The software Flow EFD 16 (Siemens) was used for processing gas flow field and pressure profiles by solving the viscous laminar compressible Navier-Stokes equations. The initial conditions were the atmospheric pressure and typical flow rate of 10 $l.min^{-1}$ at the output of the pyrolysis reactor and a flow rate of 0.120 $l.min^{-1}$ at the outlet of the

sampling stage, which is determined by the sample conditioning system. After solving the flow profile, spherical particles of different sizes and densities were injected downstream of the flow control orifice into the gas flow field, and their trajectories were calculated with the Lagrangian approach. One thousand particle trajectories for each particle type and aerodynamic condition were processed (Figure 2). Their initial radial positions were set randomly and homogeneously distributed on a perpendicular-to-axis plane of the mainstream flow from the reactor.

The calculated loss of particles during the sampling stage was less than 0.1% for any size between 1 and 100 nm, with a dilution range of 50% (Fig 2a) to 90% (Fig 2b). The density of the particles was assumed to be equal to unity as it represents the worst case in terms of particle loss. This was qualitatively in good agreement with experimental results in which very few depositions were observed in the dilution chamber after continuous work for several hours. The particle flow was then driven to the sample conditioning and analysis parts through a 6 mm internal diameter and 10 m long tube.

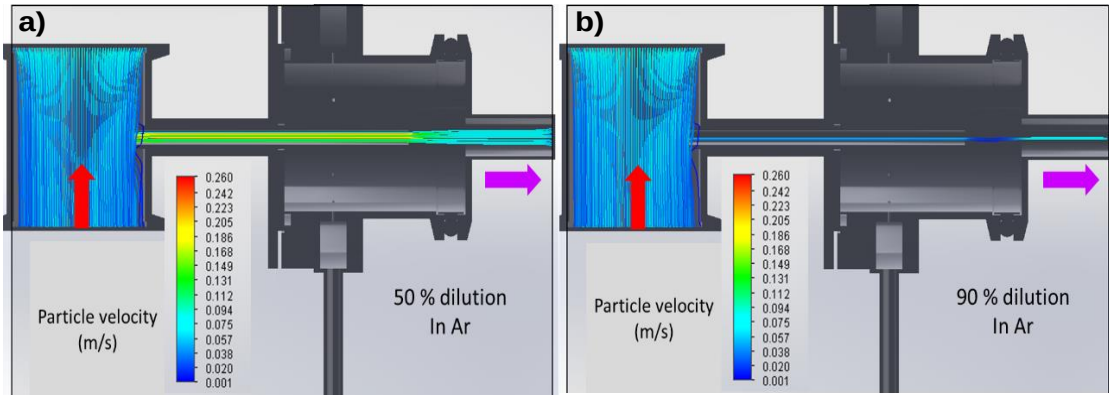

Figure 2: Particle trajectory CFD calculations in the sampling stage for a) 50% dilution in Ar and b) 90% dilution in Ar.

3.2 SAMPLE CONDITIONING: AERODYNAMIC LENS SYSTEM

The sample conditioning stage was designed to produce a thin, collimated beam of isolated particles under vacuum from an aerosol sample at atmospheric pressure. Decisive advantages of this design were expected: first, working under vacuum conditions eliminates the background emission signal from any gaseous components in the analysis stage. Second, the thin and collimated beam of isolated particles ensures a high density of particles in the laser-sample interaction volume to be analyzed. Densities of up to 10^7 cm^{-3} were previously measured in the beam with a classical aerosol generator as a particle source [25]. Third, as the particles are isolated, it is possible to adjust the analysis parameters to have, at the most, one particle in the laser focal volume statistically. This leads to the possibility to analyze a single particle (section 4.2.2). Fourth, analysis under a vacuum environment might facilitate the LIBS analysis of elements emitting in the UV range, even giving access to VUV measurements. Globally, conditioning the sample should lead to a dramatic increase in the sensitivity of the analysis of particles in the gas phase.

The conditioning of the sample in a nanoaerosol jet was achieved with an aerodynamic lens system [26]. Such a setup has been commonly used in different analytical techniques such as Time-of-Flight Mass Spectrometry [27] or X-ray Photoelectron Spectroscopy on isolated nanoparticles [28]. Furthermore, it has also been successfully applied to particle detection using Laser-Induced Breakdown Detection (LIBD) [25].

The aerodynamic lens systems are usually composed of 3 parts: a flow control orifice, an aerodynamic focusing stage, and an acceleration nozzle. The flow control orifice adjusts the gas volume flow rate throughout the system. In this work, we used a plane geometry at the entrance, with a 3 mm long conical outlet (half-angle of 45°) and 200 µm diameter, resulting in a volume flow rate of 0.120 $l.min^{-1}$ of Ar introduced in the lens system.

Our aerodynamic focusing stage consisted of a series of 4 elementary lenses. The cylindrical chamber dimensions were 10 mm (diameter) by 50 mm (length), except for the last one, which had a length of 70 mm. The stage began with an inlet capillary-like diaphragm of 5 mm in diameter. Subsequently, the diaphragm diameters of the focusing stage decreased progressively from the inlet to the outlet, as 4.75 mm, 4.5 mm, 4.25 mm, and 4 mm, respectively. The inlet and the last capillary-like diaphragms were 20 mm long, while the others were constructed using 0.5 mm thick plates. The acceleration nozzle was used as an outlet of the system to vacuum (4 mm diameter). Overall, the aerodynamic lens system demonstrated an exceptionally high transmission capability over a wide range of particle sizes, allowing long term use [26].

3.3 Sample Analysis

At the aerodynamic lens outlet, the particle flow was introduced in the analysis chamber as a thin, dense, and collimated beam. The pressure in this chamber was maintained around 0.5 mbar by a primary roots pump of Pfeiffer ACP 40 type. A sectional view of this chamber is given in Figure 3. The particle beam is introduced vertically from the top and passes through a 1 mm internal diameter skimmer before arriving in the laser interaction chamber. The pressure in this chamber is maintained at 10^{-2} mbar by an additional primary root pump (Pfeiffer ACP 40). The distance between the aerodynamic lens outlet and the skimmer was 10 mm, and the distance between the skimmer and the interaction zone was 20 mm.

A 5 kHz Technifor laser (300 µJ per pulse, 5 ns pulse duration) was used as the laser source at 1064 nm wavelength. The laser beam was focused using a x10 Thorlabs objective (LMH-10x-1064), with a working distance of 11 mm. The plasma light was collected directly using a 600 µm core diameter optical fiber with a numerical aperture of 0.22 and placed at 4 mm from the laser-particle interaction area. The fiber was coupled to a Czerny-Turner spectrograph with a 1200 $lines.mm^{-1}$ grating blazed at 300 nm (Princeton Instruments SP2300i) with an ICCD detector (DH740 IStar Andor). The synchronization of the laser and the detector was conducted with a delay generator. The interaction region was visually monitored with an optical camera to facilitate the alignment of the laser with the particle beam using XYZ micrometric manual stages.

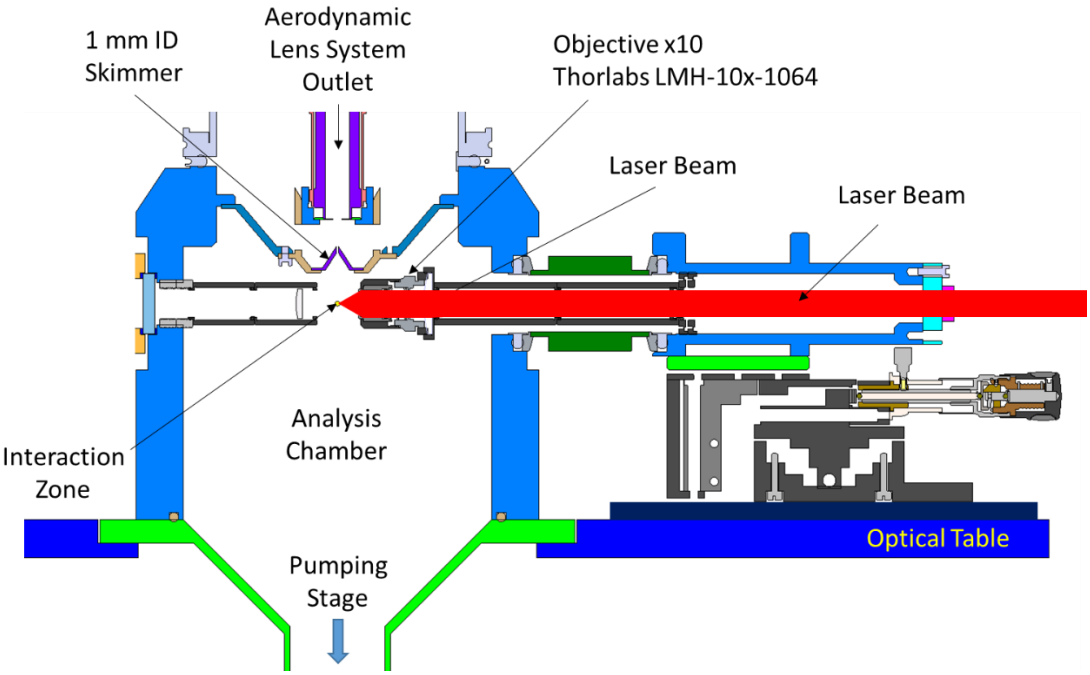

Figure 3: Sectional view of the Analysis chamber.

4 RESULTS AND DISCUSSION

For practical reasons linked to experimental time constraints during the analysis of particles generated by the laser pyrolysis reactor, preliminary tests were performed from an atomized suspension of particles. The goal of these preliminary tests is to optimize the LIBS temporal parameters and laser energy for further evaluation of the performance and efficacy of the analysis system and sample conditioning stage in a representative and known set of experimental conditions [29].

4.1 SETTING OF LIBS PARAMETERS

The preliminary tests were performed using Si nanoparticles of 100 nm diameter suspended in ethanol. The colloidal suspension was nebulized using an aerosol generator, Palas AGK2000, generating droplets with average diameters ranging from 2 to 3 µm, and Ar as the carrier gas. Their suspension in ethanol was stable with a concentration of 0.5 $g.l^{-1}$. After atomization, the solvent removal from the droplets was done by simple evaporation before the aerosol reached the lens system's entrance orifice. To achieve this, the choice of ethanol was deliberate because of its rapid evaporation kinetics. Additionally, we incorporated a 50 cm-length buffer tube (2.5 cm in diameter) between the aerosol generator and the critical orifice to guarantee ethanol's complete evaporation before the aerosol's entrance into the aerodynamic lens system.

First, an appropriate optimization of laser energy and acquisition integration time was necessary to achieve optimal results. Figure 4a shows the net integrated signal of the Si I line lying at 288.16 nm as a function of the laser pulse energy. The energy threshold was found to be 155 µJ/pulse for Si particles, estimated using the linear response range of the curve and fixing the null value as 3 times the standard deviation of the background. The relative stabilization of the analytical signal from 250 µJ suggests that particles interacting with the laser are fully vaporized at energy levels exceeding this value. Furthermore, it could be also seen an increase in signal attributable to more intense heating of the plasma by the fraction of laser energy not consumed in vaporizing the

particle. Therefore, for subsequent experiments, the laser energy was set at a fixed value of 350 µJ per pulse, operating at a frequency of 5000 Hz.

The temporal evolution of the Si I emission can be observed in Figure 4b. The emission becomes negligible after 450 ns. As known, the delay/integration times optimization on LIBS experiment is a critical aspect. Due to the weak signal intensity and the negligible continuum emission thanks to working under vacuum conditions, we selected an integration time of 1 µs to ensure the total collection of the plasma emission, beginning at t=0 ns. The average signal and the standard deviation values correspond to 5 repetitions of 25000 accumulation series.

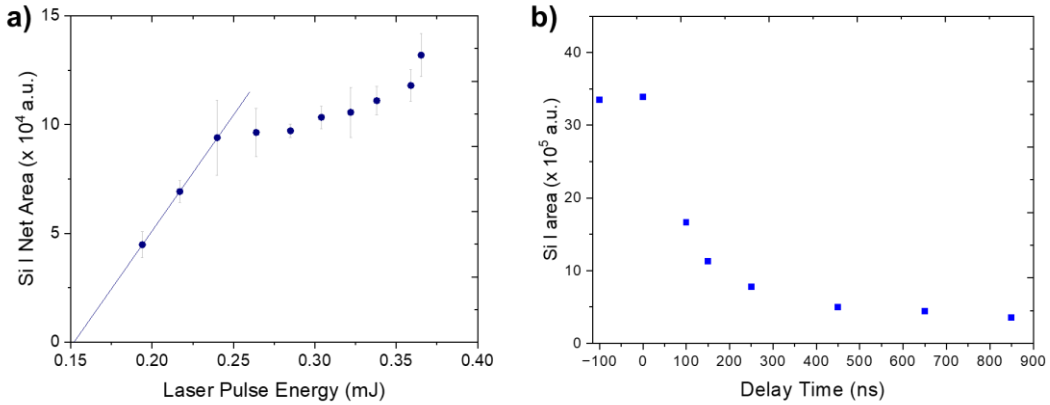

Figure 4: a) Evolution of the Si emission line area as a function of the laser pulse energy. b) Evolution of the Si emission line area as a function of the delay time from the laser emission at 350 µJ/pulse (integration time 1 µs).

4.2 ONLINE NANOAEROSOLS ANALYSIS USING LIBS

After optimizing the LIBS parameters, we conducted online analysis experiments with the laser-based pyrolysis synthesis system as the aerosol source to validate the experimental setup under a complete gas-phase environment (laser pyrolysis setup), with particles of complex elemental composition. The aerosol generator used in the previous section was removed, while the sampling system described in the experimental section (section 3.1) was installed. The implementation of this sampling system allowed us to carry out the proof-of-concept for the instrumental design and the methodological process required for future online analysis of nanoaerosols.

As previously exposed, the sampling system was designed to collect particles in the gas phase and dilute them due to their high concentration in the synthesis system. An Argon (Ar) flow of 40 sccm was introduced to prevent system clogging, resulting in an 80% dilution rate in the main channel to the aerodynamic lens system, as confirmed by CFD calculations.

Considering the different atomic emissions of the three elements (Li, Ti, and O) from Li_2TiO_3 particles, as well as the varying spectral sensitivity of our detection system at the corresponding wavelengths, we optimized the gain level to achieve a compromise between the signal levels and the saturation of the CCD for each case. Three spectral windows were chosen using a 1200 lines/mm grating, centered at different spectral regions to detect Li I at 670.8 nm, Ti II lines around 335 nm, and O I at 777.4 nm.

Two different acquisition modes were used to record LIBS signals from the particles. In the first one, called "*accumulation mode*" the signal from all laser shots was accumulated on the CCD during a fixed exposure time. This mode was supposed to be convenient to get an average estimation of the relative proportion of each element. In the second one, called "single event mode", the CCD was synchronized and temporally

gated to acquire the signal from a single laser shot. This mode was supposed to allow the analysis of a single event.

4.2.1 Results in the accumulation mode

The measure mode was fixed as accumulation on-CCD mode with an exposure time of 35 ms, i.e. 175 accumulated laser shots at a 5 kHz repetition rate. The number of spectra for each spectral region varied between 6000 and 8000 due to the time constraint induced by the laser pyrolysis system.

Given the discrete nature of LIBS events, it was crucial to distinguish between the events in which the laser has interacted with a particle and generated a plasma (hits); and background signals (no-particle events) for each acquisition. As consequence, a *hit* was defined as a spectrum exhibiting a statistically significant signal of an element compared to the background. To distinguish between a hit and the background, a *data conditional analysis* was applied based on the work of J.E. Carranza et al. [17]. The idea behind this treatment is to compare the analytical signal of the emission lines of the analyte of interest (in our case, the integrated signal) with the analytical signal selected in a neighbor spectral region without emission lines (called *"Peak Off"* region). A spectrum was classified as a *hit* if the analytical signal exceeds a threshold value, set as the percentile 99.5% of the peak-off data.

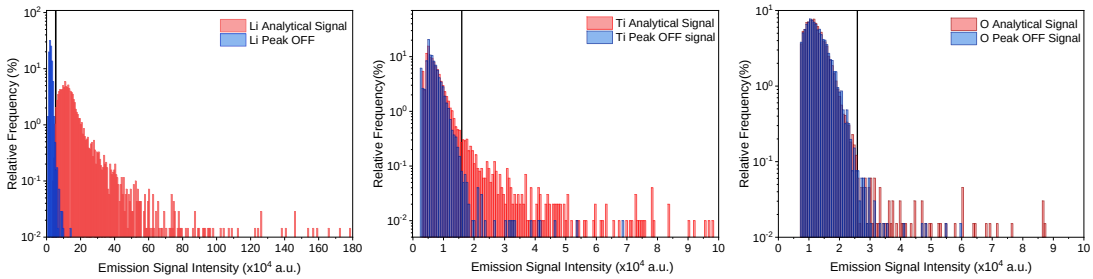

Figure 5: Histograms for the recorded signals and the background for Li, Ti and O from Li_2TiO_3 particles. The analytical signal (hit) is in red and background signal (peak off) is in blue. The proportion of hits is much higher for Li than for Ti and O.

The histograms in Figure 5 present the analytical signals from the emission lines of the three considered elements. The regions of the spectra selected as analytical signals where the most intense emission lines were located (334.9 for Ti II, 670.8 nm for Li I, and the triplet 777.1, 777.4, and 777.9 nm for O I).

The black vertical lines in Figure 5 represent the threshold value on the "peak off" data. Furthermore, as observed on the histograms represented in Figure 5, the threshold values and the hit rate in each element are not the same, as it depends on the sensitivity of the LIBS technique to each one and on the selected emission line. Therefore, the individual values must be optimized individually. The rate of hits was 98.5 %, 5.5 %, and 1.17% for Li, Ti, and O, respectively.

Furthermore, the measurements were repeated during the same laser pyrolysis experiment to check changes in the hit detection capabilities, and the new percentages obtained were 97.3 %, 3.9 %, and 1.2 % (Li, Ti, and O, respectively), proving that the system provides reproducible results. The high ratio of Li hit-event detected demonstrates the high sensitivity of the system to detect particles from light elements, providing the capability to make online monitoring of gas-phase synthesis processes.

Considering the hit rate as a proxy of the measurement sensitivity, in our experimental conditions the sensitivity for Li is ~80 times higher than that of O and ~20 times higher

than that of Ti. Those ratios can be used to estimate the average plasma temperature, based on the Boltzmann equation describing the line intensity of an element X at wavelength λ and temperature T (in eV):

$$I(X,\lambda,T) = F(\lambda)N_X \frac{hc}{\lambda}\frac{gA}{Z(T)} exp\left(-\frac{E_{up}}{T}\right)$$

With F(λ) the instrumental spectral efficiency, N_X the number of emitting atoms, h the Planck constant (J.s), c the speed of light (m/s), g the degeneracy level of the transition, A the transition probability (s^{-1}), Z(T) the partition function of the species, E_{up} the energy of the upper level of the transition (eV). Given the stoichiometry of Li_2TiO_3 nanoparticles and the relative spectral efficiency of our experimental setup at the three wavelengths of interest, the experimental Li/O and Li/Ti sensitivity ratios lead to an average plasma temperature of ~1.35 eV. Although the local thermodynamic equilibrium hypothesis, required to apply the Boltzmann equation, is not fulfilled in our case due to vacuum conditions and to the time integration of spectral measurements, this temperature is consistent with previous works on LIBS analysis of solids under vacuum [30,31]. Reciprocally, this opens up perspectives on quantitative analysis of the particle's composition based on a calibration-free approach, which requires the determination of the plasma temperature [32].

The different sensitivity from Ti II and O I, being lower than that of Li, leads to noisier signals in the median spectrum without additional data treatments, as a conclusion from Figure 5. The need to perform conditional analysis is obvious when comparing the average spectra of all the complete data set of the analyzed spectra (raw data) with those that meet the Data Conditional Analysis criteria, as depicted in Figure 6. While the difference was very small for Li, this treatment was necessary to detect Ti and O, otherwise the corresponding spectra would not have emerged from the background, hindering their correct identification.

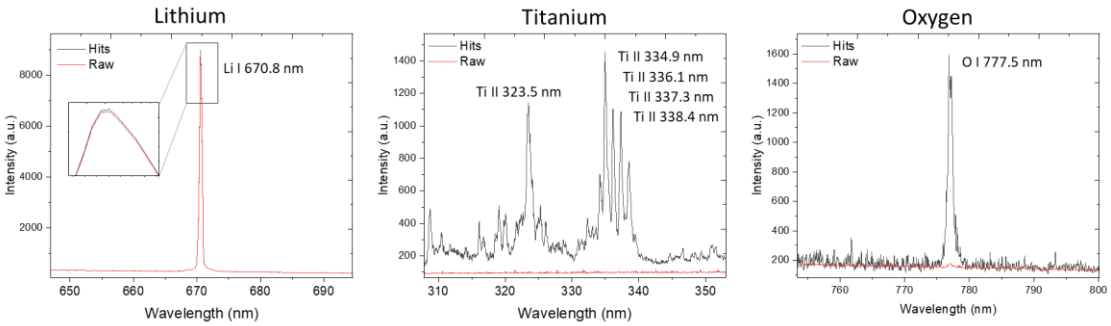

Figure 6: Comparison between the spectra obtained by the mean of all the data set (Raw data in red) with those obtained only considering the hits event for the 3 spectral regions analyzed.

Furthermore, a 5 kHz repetition rate laser has ensured the quasi-real-time monitoring capability of the nanoparticles composition. Concerning the Ti results, which were clearly not as favorable as in the case of Li, one hit was obtained every 24 spectra on average (± 29 spectra), i.e. 840 ms, as presented in Figure 7. The LIBS acquisition system presented in this work would provide analytical information in less than 1 s with current acquisition conditions, while there was a probability of 95 % to obtain one hit in less than 2 s. As several hits are necessary to get a statistically satisfying signal, we consider that a real-time monitoring of the relative stoichiometry of Li_2TiO_3 particles for Li and Ti during their synthesis in the gas phase is possible within a time constant of 10 s. In addition, an

absolute stoichiometry control should also be possible with an adequate calibration (which could not be achieved in this preliminary work).

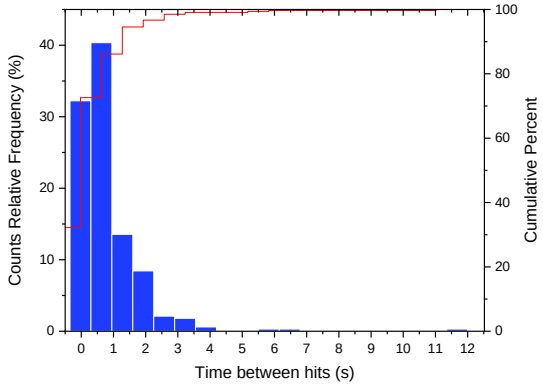

Figure 7: Histogram (blue, left axis) and cumulative probability (red, right axis) for the time lapses between 2 consecutive hits during the Ti II measurement.

4.2.2 Results in the single event acquisition mode

Using the Li emission signal, a series of 10 000 single laser-pulse spectra was recorded without any accumulation on the CCD. Only the signal from a single laser shot is recorded at a time. In this case, the acquisition speed was limited by the ICCD response time, and the hit rate for Li was reduced to 4.7%. It means that at least one particle is localized in the laser focal volume every 21 laser shots. Assuming Poisson statistics, the probability of having more than one particle in the focal volume during a laser shot is then negligible. Thus, the ability to detect the emission from the interaction of one laser shot and a single event is demonstrated.

Concerning the signal amplitude of events, a small part of them is recorded with a level higher than the median analytical signal of the hit events plus 3 times the standard deviation (Figure 8a). These events were attributed to casual aggregates. Figure 8b shows the median spectrum in single event compared to the accumulation mode. In both cases, the Li emission line is perfectly appreciable. The difference in intensity between both spectra is due to the accumulation. The capability to carry out single-event LIBS at a high laser repetition rate might increase the field of applications of this technique since when considering a single event, the spectral signal will be given by the particle size, while the hit rate will give information about the number concentration of the particles.

Considering the density of 3430 kg/m^3 of Li_2TiO_3, the size of 120 nm of particles and that Li is representing only 5% of the mass of Li_2TiO_3, we can set a detection limit of approximately 150 ag for Li with this technique, which is very low. This performance is in accordance with a laser-particle interaction under vacuum with no background from the surrounding gas, reduced spectral lines broadening and a non-confined plasma from an isolated particle, leading to an efficient excitation conversion and a very high resulting sensitivity.

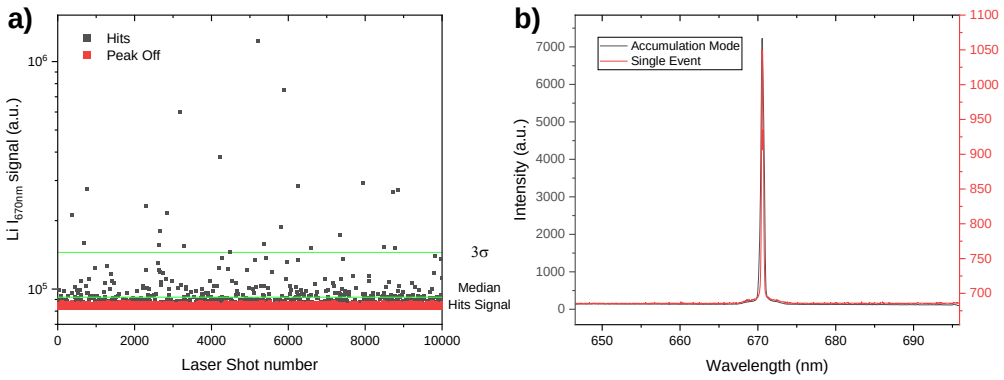

Figure 8: a) Li I emission intensity at 670 nm for the single event detection, representing in red the hits, in black the background, and the mean and standard deviation for the hits set. b) Comparison between the accumulation mode (Black line, left axis) and the single event mode (red line, right axis)

5 CONCLUSIONS

This work presents a new process for the direct and real-time analysis of nanoaerosols by LIBS coupled to an aerodynamic lens system. By combining this powerful LIBS analysis method with the laser pyrolysis synthesis process, we have established a groundbreaking approach to studying and characterizing nanoparticles in real-time throughout their formation. This integration of continuous analysis and particle synthesis holds a paramount potential for advancing nanomaterial research and development across various fields of science and engineering.

The instrument is composed of three parts. First, a sampling stage allows the continuous injection of a part of the particles at the outlet of the synthesis process with a control of the concentration of the injected particles with a dilution system. Second, a conditioning stage transforms the selected aerosol sample into a collimated beam of nanoparticles under 10^{-2} mbar pressure with an aerodynamic lens system. Third is the analysis stage, where the particle jet and the laser interact. It was designed to conduct LIBS analysis, taking advantage of the low working pressure and high aerosol concentration from the aerodynamic lens system. This leads to decisive benefits such as reducing the spectral lines broadening, increasing the spectral resolution, and reducing the continuum coming from the laser-plasma interaction.

The efficiency of the device was evaluated with an aerosol generator to establish the appropriate time and energy frames for analyzing nanoparticles at low pressure. For the measured Si particles, the laser-induced plasma emission duration was characterized as lower as 500 ns without any significant continuum emission. The laser/particle interaction under vacuum leads to a fast-expanding plasma corresponding to a complete breakdown of the small particle and a probable isotropic optical emission. The ablation of the particles with pulse energy in the order of only 150 µJ was also demonstrated with a signal 3 times higher than the standard deviation of the background level.

Furthermore, a new proof-of-concept was carried out by online monitoring the relative elemental composition of Li_2TiO_3 nanoparticles during their synthesis in the gas phase by laser pyrolysis. First, we have conducted the measurement of Li, Ti, and O, simultaneously to the nanoparticle synthesis and successfully implemented the data conditional analysis method in our experiment. The results allowed us to quickly

differentiate between the hits (spectra with analytical information) and the background, obtaining the characteristic spectral signature of the 3 elements under study. In addition, the measurements were repeated with comparable results. Finally, our experimental setup allowed us to obtain exploitable results in less than 10 s, which makes it an excellent candidate to perform real-time analysis. Finally, we performed single-particle LIBS analysis thanks to the use of a kHz repetition rate laser with a detection limit of the order of 150 ag for lithium.

This novel approach presents great potential for the analysis of nanoaerosols, not only in the industrial field of online control of synthesis processes but also for the monitoring of outdoor or indoor atmospheric particles.

6 ACKNOWLEDGEMENTS

The authors would like to acknowledge the funding of the ALNIV project by the Labex PALM et NanoSaclay program from 'Université Paris-Saclay..

7 DECLARATION OF COMPETING INTEREST

The authors declare that they have no known competing financial interests or personal relationships that could have appeared to influence the work reported in this paper.

8 BIBLIOGRAPHY

[1] E. Pomerantseva, F. Bonaccorso, X. Feng, Y. Cui, and Y. Gogotsi, "Energy storage: The future enabled by nanomaterials," *Science (1979)*, vol. 366, no. 6468, p. eaan8285, Nov. 2019, doi: 10.1126/science.aan8285.

[2] W. Gao and L. Zhang, "Nanomaterials arising amid antibiotic resistance," *Nat Rev Microbiol*, vol. 19, no. 1, pp. 5–6, Jan. 2021, doi: 10.1038/s41579-020-00469-5.

[3] D. R. Baer and M. H. Engelhard, "XPS analysis of nanostructured materials and biological surfaces," *J Electron Spectros Relat Phenomena*, vol. 178–179, pp. 415–432, May 2010, doi: 10.1016/j.elspec.2009.09.003.

[4] B. Meermann and V. Nischwitz, "ICP-MS for the analysis at the nanoscale – a tutorial review," *J Anal At Spectrom*, vol. 33, no. 9, pp. 1432–1468, 2018, doi: 10.1039/C8JA00037A.

[5] E. S. Galvão, J. M. Santos, A. T. Lima, N. C. Reis, M. T. D. Orlando, and R. M. Stuetz, "Trends in analytical techniques applied to particulate matter characterization: A critical review of fundaments and applications," *Chemosphere*, vol. 199, pp. 546–568, May 2018, doi: 10.1016/j.chemosphere.2018.02.034.

[6] F. Taccetti, L. Castelli, C., Czelusniak, *et al.*, A multipurpose X-ray fluorescence scanner developed for in situ analysis. Rend. Fis. Acc. Lincei 30, 307–322 (2019). https://doi.org/10.1007/s12210-018-0756-x

[7] M.R. Stolzenburg, and P.H. McMurry, Method to assess performance of scanning mobility particle sizer (SMPS) instruments and software, Aerosol Science and Technology (2018) 52(6), 609–613. https://doi.org/10.1080/02786826.2018.1455962

[8] D. W. Hahn and N. Omenetto, "Laser-Induced Breakdown Spectroscopy (LIBS), Part I: Review of Basic Diagnostics and Plasma–Particle Interactions: Still-Challenging Issues Within the Analytical Plasma Community," *Appl Spectrosc*, vol. 64, no. 12, pp. 335–366, Dec. 2010, doi: 10.1366/000370210793561691.

[9] D. W. Hahn and N. Omenetto, "Laser-induced breakdown spectroscopy (LIBS), part II: review of instrumental and methodological approaches to material analysis and applications to different fields.," *Appl Spectrosc*, vol. 66, no. 4, pp. 347–419, May 2012, doi: 10.1366/11-06574.

[10] A. J. Effenberger and J. R. Scott, "Effect of atmospheric conditions on LIBS spectra," *Sensors*, vol. 10, no. 5, pp. 4907–4925, May 2010, doi: 10.3390/s100504907.

[11] C. Dutouquet *et al.*, "Monitoring of heavy metal particle emission in the exhaust duct of a foundry using LIBS," *Talanta*, vol. 127, pp. 75–81, 2014, doi: 10.1016/j.talanta.2014.03.063.

[12] C. Alvarez-Llamas, C. Roux, and O. Musset, "A compact, high-efficiency, quasi-continuous wave mini-stack diode pumped, actively Q-switched laser source for laser-induced breakdown

spectroscopy," *Spectrochim Acta Part B At Spectrosc*, vol. 148, no. February, pp. 118–128, Oct. 2018, doi: 10.1016/j.sab.2018.06.012.

[13] R. C. Wiens *et al.*, "Compositionally and density stratified igneous terrain in Jezero crater, Mars," *Sci Adv*, vol. 8, no. 34, Aug. 2022, doi: 10.1126/sciadv.abo3399.

[14] L. J. Radziemski, T. R. Loree, D. A. Cremers, and N. M. Hoffman, "Time-resolved laser-induced breakdown spectrometry of aerosols," *Anal Chem*, vol. 55, no. 8, pp. 1246–1252, Jul. 1983, doi: 10.1021/ac00259a016.

[15] D. W. Hahn, W. L. Flower, and K. R. Hencken, "Discrete Particle Detection and Metal Emissions Monitoring Using Laser-Induced Breakdown Spectroscopy," *Appl Spectrosc*, vol. 51, no. 12, pp. 1836–1844, Dec. 1997, doi: 10.1366/0003702971939659.

[16] J. E. Carranza, B. T. Fisher, G. D. Yoder, and D. W. Hahn, "On-line analysis of ambient air aerosols using laser-induced breakdown spectroscopy," *Spectrochim Acta Part B At Spectrosc*, vol. 56, no. 6, pp. 851–864, Jun. 2001, doi: 10.1016/S0584-8547(01)00183-5.

[17] J. E. Carranza, K. Iida, and D. W. Hahn, "Conditional data processing for single-shot spectral analysis by use of laser-induced breakdown spectroscopy.," *Appl Opt*, vol. 42, no. 30, pp. 6022–6028, 2003, doi: 10.1364/AO.42.006022.

[18] V. Hohreiter and D. W. Hahn, "Plasma-particle interactions in a laser-induced plasma: Implications for laser-induced breakdown spectroscopy," *Anal Chem*, vol. 78, no. 5, pp. 1509–1514, 2006, doi: 10.1021/ac051872s.

[19] J. E. Carranza and D. W. Hahn, "Assessment of the Upper Particle Size Limit for Quantitative Analysis of Aerosols Using Laser-Induced Breakdown Spectroscopy," *Anal Chem*, vol. 74, no. 21, pp. 5450–5454, Nov. 2002, doi: 10.1021/ac020261m.

[20] J. E. Carranza and D. W. Hahn, "Plasma volume considerations for analysis of gaseous and aerosol samples using laser-induced breakdown spectroscopy," *J Anal At Spectrom*, vol. 17, no. 11, pp. 1534–1539, Nov. 2002, doi: 10.1039/b206140f.

[21] F. J. Fortes, A. Fernández-Bravo, and J. Javier Laserna, "Chemical characterization of single micro- and nano-particles by optical catapulting-optical trapping-laser-induced breakdown spectroscopy," *Spectrochim Acta Part B At Spectrosc*, vol. 100, pp. 78–85, 2014, doi: 10.1016/j.sab.2014.08.023.

[22] T. Amodeo *et al.*, "On-line monitoring of composite nanoparticles synthesized in a pre-industrial laser pyrolysis reactor using Laser-Induced Breakdown Spectroscopy," *Spectrochim Acta Part B At Spectrosc*, vol. 63, no. 10, pp. 1183–1190, Oct. 2008, doi: 10.1016/j.sab.2008.09.005.

[23] O. Sublemontier *et al.*, "Synthesis and On-line Size Control of Silicon Quantum Dots," *KONA Powder and Particle Journal*, vol. 29, pp. 236–250, 2011, doi: 10.14356/kona.2011024.

[24] G. Wattieaux *et al.*, "On Line Characterization of SiC Nanoparticles Produced by Laser Pyrolysis," *J Phys Conf Ser*, vol. 304, p. 012021, Jul. 2011, doi: 10.1088/1742-6596/304/1/012021.

[25] F.-A. Barreda *et al.*, "In-situ characterization of nanoparticle beams focused with an aerodynamic lens by Laser-Induced Breakdown Detection," *Sci Rep*, no. October 2015, pp. 1–7, 2015, doi: 10.1038/srep15696.

[26] P. Liu, P. J. Ziemann, D. B. Kittelson, and P. H. McMurry, "Generating Particle Beams of Controlled Dimensions and Divergence: II. Experimental Evaluation of Particle Motion in Aerodynamic Lenses and Nozzle Expansions," *Aerosol Science and Technology*, vol. 22, no. 3, pp. 314–324, Jan. 1995, doi: 10.1080/02786829408959749.

[27] J. T. Jayne *et al.*, "Development of an Aerosol Mass Spectrometer for Size and Composition Analysis of Submicron Particles," *Aerosol Science and Technology*, vol. 33, no. 1–2, pp. 49–70, Jul. 2000, doi: 10.1080/027868200410840.

[28] O. Sublemontier *et al.*, "X-ray Photoelectron Spectroscopy of Isolated Nanoparticles," *J Phys Chem Lett*, vol. 5, no. 19, pp. 3399–3403, Oct. 2014, doi: 10.1021/jz501532c.

[29] J. Picard, J.-B. Sirven, and O. Sublemontier, "On-line Monitoring of Nanoparticle Synthesis by Laser-Induced Breakdown Spectroscopy in Vacuum," *MRS Adv*, vol. 2, no. 28, pp. 1487–1491, Jun. 2017, doi: 10.1557/adv.2016.633.

[30] I.B. Gornushkin et al. "Experimental verification of a radiative model of laser-induced plasma expanding into vacuum," *Spectrochim Acta Part B At Spectrosc*, vol. 60, no. 2, pp. 215-230, 2005, doi: 10.1016/j.sab.2004.11.009.

[31] P. Veis, A. Marín-Roldan and J. Krištof "Simultaneous vacuum UV and broadband UV–NIR plasma spectroscopy to improve the LIBS analysis of light elements" *Plasma Sources Sci. Technol*, vol. 27, pp. 095001, Sept. 2018, doi: 10.1088/1361-6595/aad668.

[32] J. Hermann et al. "Progress in calibration-free laser-induced breakdown spectroscopy" *Spectrochim Acta Part B At Spectrosc*, vol. 200, pp. 106595, 2023, doi: 10.1016/j.sab.2022.106595